Executive summary
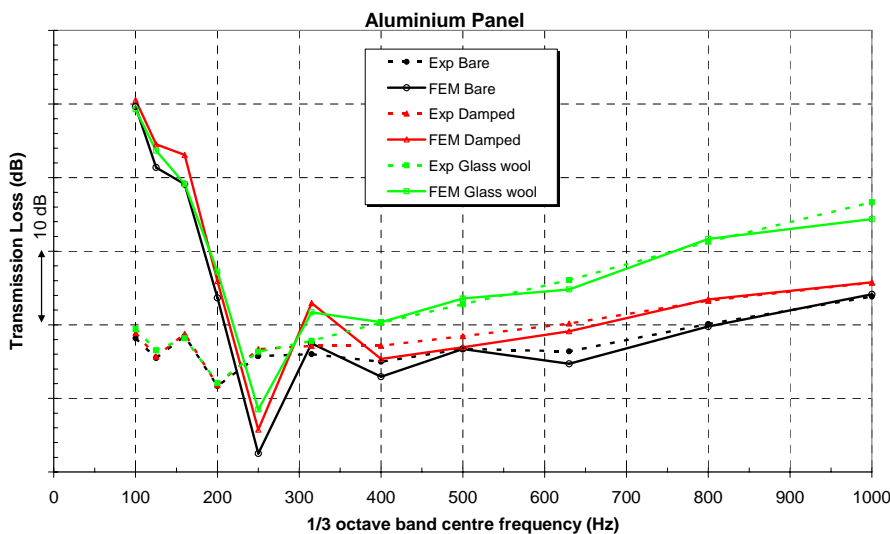
Transmission Loss analyses on fuselage panels

Approach, numerical results and validation

Description of work

A new approach has been presented in detail to solve structural-acoustic problems. The structure as well as the fluid is modelled with the Finite Element Method. The new approach reduces the computational effort compared with a more conventional FEM approach. This is necessary in case of large models, existing for realistic aircraft structures such as fuselage panels or even a fuselage barrel, which are the structures analysed within the framework of the EU-project FACE. The main objective here was to predict the sound transmission (TL) through these realistic aircraft fuselage panels.

Results and conclusions

Results obtained with this approach are presented for a bare, damped (viscous constraining layer) and furnished (glass wool) large Aluminium fuselage panel configuration. The results have been compared with experimental data (modal and TL-data), validating the approach.

For the Aluminium fuselage panel the correlation with the experimental transmission loss results is excellent for frequencies above the 350 Hz (less than 2 dB differences). Below the 350 Hz, a much higher TL is predicted in the numerical analyses. This can be due to the Rigid body modes.

This report is based on a presentation to be held at ISMA 2006 International Conference on Noise and Vibration Engineering, Leuven, Belgium, 18-20 September 2006

Similar results have been obtained for a Composite fuselage panel, although the correlation with experimental TL results was somewhat less than for the Aluminium panel, but still good for frequencies above the 400 Hz.

NLR-TP-2006-479

Transmission Loss analyses on fuselage panels
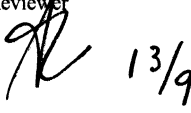
Approach, numerical results and validation

F.P. Grooteman

Customer	European Union
Contract number	G4RD-CT2002-00764
Owner	National Aerospace Laboratory National Aerospace Laboratory NLR
Division	Aerospace Vehicles
Distribution	Unlimited
Classification of title	Unclassified

Approved by:

Author	Reviewer	Managing department

Summary

In this paper a new solution strategy will be presented to solve structural-acoustic problems in a more efficient way. Both the structure and fluid domain are modelled with the Finite Element Method (FEM). The new approach reduces the computational effort compared with the more conventional FEM approach, by introducing non-coinciding fluid and structure mesh and separate solution of both domains, but in a fully coupled fashion. This is necessary in case of large models, existing for realistic aircraft structures such as fuselage panels or a fuselage barrel, which are the type of structures analysed within the framework of the European programme FACE (Friendly Aircraft Cabin Environment). One of the main objectives within this project was to predict the sound transmission through aircraft fuselage panels.

The solution strategy has been implemented in the in-house finite element program B2000. Numerical results obtained for a large Aluminium fuselage panel are presented and compared with experimental data (modal and transmission loss data) to validate the approach. The following panel configurations have been analysed: bare, damped (viscous constraining layer) and furnished (glass wool).

Contents

Transmission Loss analyses on fuselage panels: approach, numerical results and validation

F.P. Grooteman

National Aerospace Laboratory, Aerospace Vehicles Division
Anthony Fokkerweg 2, 1059 CM, Amsterdam, The Netherlands
email: grooten@nlr.nl

Abstract

In this paper a new solution strategy will be presented to solve structural-acoustic problems in a more efficient way. Both the structure and fluid domain are modelled with the Finite Element Method (FEM). The new approach reduces the computational effort compared with the more conventional FEM approach, by introducing non-coinciding fluid and structure mesh and separate solution of both domains, but in a fully coupled fashion. This is necessary in case of large models, existing for realistic aircraft structures such as fuselage panels or a fuselage barrel, which are the type of structures analysed within the framework of the European programme FACE (Friendly Aircraft Cabin Environment). One of the main objectives within this project was to predict the sound transmission through aircraft fuselage panels.

The solution strategy has been implemented in the in-house finite element program B2000. Numerical results obtained for a large Aluminium fuselage panel are presented and compared with experimental data (modal and transmission loss data) to validate the approach. The following panel configurations have been analysed: bare, damped (viscous constraining layer) and furnished (glass wool).

1 Introduction

The field of acoustics is of interest in various types of industries, for example the automobile, aircraft and space industry. This is due to the ongoing optimisation of structures resulting in lighter stiff structures, which are more vulnerable for vibrations, as well as the increase in demand for environmental friendlier structures and passenger comfort.

Passenger comfort in aircraft has been an important research topic over the past decades. A low noise environment is an important issue for airline operators and passengers for new generations of aircraft. Main part of the interior noise is caused by external noise sources, such as engines and boundary layer noise, which transmit through the fuselage structure.

The fuselage structure is essentially a double wall system consisting of the stiffened outer shell, the inner trim panels mounted to the stiffeners and in between a cavity partly filled with insulation material and air, schematized in figure 1.1. A good numerical model describing the sound transmission through the aircraft fuselage, allows aircraft manufacturers to predict the noise level inside the aircraft and design more silent aircraft cabins.

One of the goals of FACE is to predict the sound transmission through real furnished aircraft fuselage panels and even a fuselage barrel. These problems result in larger finite element models. Although computer power has increased considerably over the past decades, this type of analysis still remains very time consuming requiring large computing resources.

Direct solution of the coupled structural-acoustic system of equations is difficult and time consuming, because the global matrices are non-symmetric, complex and frequency dependent, in general. Therefore one of the objectives of NLR in FACE was to develop a more efficient

solution strategy, which is discussed in detail in chapter 2. The solution strategy is based on the following considerations:

- Non-coinciding fluid and structure mesh.
  In general, the wavelengths present in the structure are much smaller than those in the fluid domain. The mesh density in the fluid domain can therefore be selected much coarser. This considerably reduces the number of degrees of freedom. Therefore, the most efficient way is to mesh the fluid and structure domain separately and allow for non-coinciding meshes at the interface.
- Separate solution of both domains, but in a fully coupled fashion.
  Solving two smaller problems is much more efficient than solving the whole problem at once, especially here, since the two smaller problems are symmetric with a much smaller bandwidth contrary to the overall problem.

This solution strategy has been implemented in the finite element program B2000 (Ref. 1), which is an open, modular finite element environment for which the source code is available (www.smr.ch) and is used at NLR as a FEM development tool.
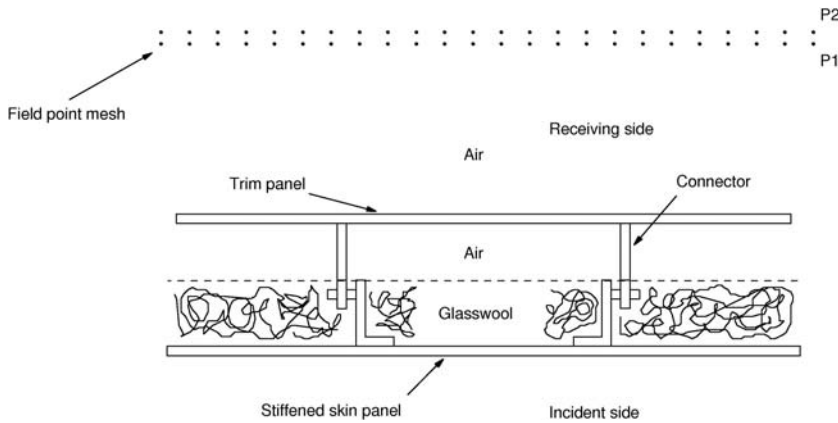
Figure 1.1: Schematised double wall set-up

In chapter 3 numerical results will be presented obtained with this new solution strategy for a bare, damped and furnished Aluminium fuselage panel. The numerical results are compared against experimental results to validate the model.

2 Numerical approach

2.1 Considerations

The dynamical behaviour of the fluid in an aircraft cabin can be described by the Helmholtz equation,

$$\nabla^2 p + k^2 p = 0 \quad ; \quad k = \omega / c \tag{1}$$

provided the following requirements are fulfilled:

- The fluid behaves inviscid, i.e. shear forces in the fluid can be neglected, which is no longer valid for very thin air layers (Ref. 2).
- The fluid behaves like an ideal gas.
- The fluid is supposed to be at rest (no mean velocity).
- Only small harmonic fluctuations around the equilibrium state are allowed.
  For very high sound pressure levels (above the threshold of pain > 130 dB) this no longer is valid.

In terms of a FEM formulation this equation, with proper boundary conditions, can be discretised yielding the matrix-vector equation:

$$(K_f - \omega^2 M_f) P = F_f \qquad (2)$$

where K_f and M_f are the fluid "stiffness" respectively "mass" matrix. P is the pressure amplitude and F the force vector due to external loading (e.g. sound source). This equation is similar as the one describing the dynamical behaviour of a structure.

In case of a coupled fluid-structure problem the resulting matrix-vector equation becomes:

$$\left(\begin{bmatrix} K_s & -C_{sf} \\ 0 & K_f \end{bmatrix} + i\omega \begin{bmatrix} D_s & 0 \\ 0 & D_f \end{bmatrix} - \omega^2 \begin{bmatrix} M_s & 0 \\ C_{fs} & M_f \end{bmatrix} \right) \left\{ \begin{matrix} U \\ P \end{matrix} \right\} = \left\{ \begin{matrix} F_s^{ext} \\ F_f^{ext} \end{matrix} \right\} \qquad (3)$$

where C_{sf} and C_{fs} are the couple matrices representing the force exerted on the structure by vibrations of the fluid and vice versa. D_s and D_f represent the viscous damping present in the structure, respectively, fluid matrix.

In general, direct solution of this system of equations is difficult and time consuming, since:

* The system is non-symmetric (individual mass and stiffness matrices are symmetric).
* The system is complex representing damping in the structure and fluid (e.g. for insulation material).
* The matrices can be frequency dependent (e.g. for insulation material).
* The matrices can become very large in case of realistic problems, having a large bandwidth.

In order to reduce the computational effort in solving the above response problem, a different solution strategy is applied here based on the following considerations:

* Non-coinciding fluid and structure mesh.
* Separate solution of both domains, but in a fully coupled fashion.
* Different storage scheme combined with iterative solvers.

2.1.1 Non-coinciding fluid and structure mesh

In general, the wavelengths present in the structure are much smaller than those present in the fluid for the same frequency range. The mesh density can therefore be much coarser in the fluid domain, which considerably reduces the number of degrees of freedom. The most efficient way is to mesh the fluid and structure domain separately and allow for non-coinciding meshes at the interface of both domains. The difference in mesh density at the interface should be taken care off. For this a new module has been implemented which automatically determines the interface for a given fluid and structure mesh. The information obtained is used to construct the couple (C_{sf} and C_{fs}) and interpolation (H_{sf} and H_{fs}) matrices between fluid and structure. Automatic generation of the fluid structure interface is necessary to prevent mistakes and laborious work.

2.1.2 Separate solution of both domains

The structure and fluid problem are solved separately, however, in a fully coupled fashion. Solving two smaller problems is much more efficient than solving the whole problem at once, especially here, since the two smaller problems are symmetric with a much smaller bandwidth contrary to the overall problem of equation 3. Furthermore, iterative instead of direct solvers can now be applied more effectively (see next sub-section), due to the symmetry of the problem and improved condition number.

The basic idea is to determine a modal basis for both the structure and fluid domain and solve the coupled problem in modal co-ordinates.

The structure's modal basis is determined for the undamped structure, yielding matrices that are symmetric, real and thus easy to solve. This is a good assumption, since the mode shapes will not be influenced much by neglecting damping. Only in cases with a strong fluid-structure coupling the coupled structure modes can differ. However, even in that case the response of the structure

for the overall system should be approximated well by a linear combination of all modes, weakening the requirement that the individual modes need to be determined very precise.

Similarly, the fluid modes are also determined for the uncoupled undamped situation. For the fluid modes things are however more complicated. The resulting modes represent the so-called **acoustic dominated modes**, which cause vibration of the structure once exited by the external loading. In general, these modes are not capable of accurately representing the fluid response for the previous **structure dominated modes**. For example, the fluid response will often be concentrated in a region close to the structure. This cannot be represented by acoustic-dominated modes, which show a response for the whole fluid domain. Since these fluid modes are important for the prediction of the response in major part of the frequency domain under view, it is necessary to adjust for it. A crude approach often applied is to determine two sets of acoustic dominated modes, one where the structure is represented by rigid walls as well as one with free surface boundary conditions. It is then assumed that a linear combination of both modal sets better represent the overall response. This however is doubtful in many applications and also requires the solution of two eigenvalue problems, instead of one.

Here a different, cheaper and much more accurate approach is followed. Since the structure dominated modes are known an accurate prediction of the fluid response can be obtained by solving the corresponding undamped response problem (see second row of equation 3):

$$(K_f - \omega_{si}^2 M_f)\phi_{fi} = \omega_{si}^2 C_{fs}\phi_{si} \tag{4}$$

This can be done efficiently by means of an iterative solver, see next sub-section.

Once a modal basis has been obtained for the fluid and structure, the coupled problem can be solved accurately and efficiently in modal co-ordinates. Since the meshes of both domains are non-coinciding on the interface, construction of the coupled system is more complicated, see section 2.2.1.

2.1.3 Different storage scheme and iterative solvers

In general, the global finite element matrices are stored in so-called skyline format, which means that only the elements of a particular row are stored from the first non-zero element in that row up to and including the diagonal element. Since these matrices are sparse and banded this, in general, is an efficient storage scheme (on disk and in memory). However, for fluid-structure problems most elements within the skyline are zero as well. This can easily be as much as 95% of the elements. For large problems, as the ones in FACE, this is a main drawback. A much better way is to store only the matrix elements unequal to zero. Here, the so-called Compressed Row Storage (CRS) scheme is applied, in which only the non-zero elements are stored together with their column number. The row number can be obtained from the skyline vector.

When direct solvers are applied a factored stiffness matrix is required. During the factorisation process the zero elements within the skyline will, in general, become non-zero and the advantage of CRS disappears, although, the advantage still remains for the non-factored matrices. This disadvantage does not occur when iterative solvers are applied. A computational expensive factorisation of the stiffness matrix is not required. The original matrices are used mainly in matrix-vector operations. For large systems iterative solvers are therefore often more efficient than direct solvers.

The fluid domain can be solved easily by means of an iterative solver. For the structure domain a serious problem arises. Since aircraft fuselages are thin walled structures they are modelled by means of shell elements. In general, these shell elements have an element stiffness matrix with a very high condition number. This is caused by the reduced integration scheme applied in the calculation of the shear part of the stiffness matrix, in order to remove the shear-locking phenomena. This prevents the use of iterative solvers, since no convergence will be obtained or only against obsessive calculation times. Recently Rong and Lu (Ref. 3) published a paper dealing with this ill-conditioned problem in a different way, which seems very promising.

2.2 Outline of approach

In this section the different steps of the solution scheme are presented in more detail. The whole scheme is subdivided into the following two main parts:

- Calculation of the response of the structure, see section 2.2.1: *steps 1 to 11*
  In this part the structure and fluid domain(s) are modelled and the response of the structure due to structure and acoustic loading is calculated. A modal approach is applied here, as discussed in the previous section, in which both the structure and fluid domains are solved separately, taking into account the correct coupling between the structure and fluid domains. Both domains can have a different mesh density. In situations where the influence of the fluid on the dynamical behaviour of the structure can be neglected, weak coupling, only the structure needs to be modelled.
- Calculation of the response of the fluid domain, see section 2.2.2: *steps 12 to 13*
  In this second step the response of the fluid domain due to the structure is calculated. Here a FEM approach is chosen, but a BEM approach can also be applied. It depends on the configuration analysed which of both approaches is more applicable.

2.2.1 Calculation of the response of the structure

1. Two separate and independent input files have to be generated that describe the structure and fluid domain, including the node number co-ordinates, element connectivity and specification of material properties, boundary conditions and loading. The fluid and structure mesh can be non-coinciding on the interface.

2. Determination of the fluid structure interface.
   The fluid-structure interface is automatically determined from the information in the two input files.

3. Construction of the couple matrices for the fluid and structure domain: C_{fs}, C_{sf}

4. Construction of the structural interpolation matrix H_{sf} with which the pressure DOFs on the interface are transformed from the fluid to the structure mesh.

$$P_s = H_{sf} P_f \tag{5}$$

5. Construction of the fluid interpolation matrix H_{fs} with which the displacement DOFs on the interface are transformed from the structure to the fluid mesh.

$$U_f = H_{fs} U_s \tag{6}$$

6. Solution of the uncoupled undamped structural eigenvalue problem for n_s modes to obtain the structural modal basis of structure dominated modes.

$$(K_s - \omega_{si}^2 M_s)\phi_{si} = 0 \quad i = 1..n_s \tag{7}$$

7. Solution of the uncoupled undamped fluid eigenvalue problem for n_f modes to obtain the fluid modal basis of fluid dominated modes.

$$(K_f - \omega_{fi}^2 M_f)\phi_{fi} = 0 \quad i = 1..n_f \tag{8}$$

8. Determination of the pressure fields due to structural dominated modes and addition to the fluid modal basis.

$$(K_f - \omega_{si}^2 M_f)\phi_{fi} = \omega_{si}^2 C_{fs} H_{fs} \phi_{si} \quad i = 1..n_s \tag{9}$$

9. Determination of the displacement fields due to fluid dominated modes and addition to the structural modal basis:

$$(K_s - \omega_{fi}^2 M_s)\phi_{si} = C_{sf} H_{sf} \phi_{fi} \quad i = 1..n_f \tag{10}$$

This response problem can be solved in modal co-ordinates, by assuming that the structure response due to fluid loading can be accurately described by a linear combination of the uncoupled structure modes.

$$(k_s - \omega_{fi}^2 m_s)Q_{si} = \phi_{si}^T C_{sf} H_{sf} \phi_{fi} \quad i = 1..n_f \tag{11}$$

10. Construct the coupled fluid-structure system of equations in modal co-ordinates.

$$\left[(k_s + c_{sf} + k_f) + i\omega(d_s + d_f) - \omega^2(m_s + c_{fs} + m_f)\right]Q = f_s + f_f \tag{12}$$

with,

$$k_{sij} = \phi_{si}^T K_s \phi_{sj} \qquad c_{sfij} = \phi_{si}^T C_{sf} H_{sf} \phi_{fj} \qquad k_{fij} = \frac{1}{\omega_i^2}\phi_{fi}^T K_f \phi_{fj} \qquad c_{fsij} = \frac{1}{\omega_i^2}\phi_{fi}^T C_{fs} H_{fs} \phi_{sj}$$

$$d_{sij} = \phi_{si}^T D_s \phi_{sj} \qquad f_{si} = \phi_{si}^T F_s^{ext} \qquad d_{fij} = \frac{1}{\omega_i^2}\phi_{fi}^T D_f \phi_{fj} \qquad f_{fi} = \frac{1}{\omega_i^2}\phi_{fi}^T F_f^{ext}$$

$$m_{sij} = \phi_{si}^T M_s \phi_{sj} \qquad\qquad\qquad\qquad m_{fij} = \frac{1}{\omega_i^2}\phi_{fi}^T M_f \phi_{fj}$$

where $i,j = 1.. \, n_s + n_f$

The multiplication with $1/\omega_i^2$ term in the above equations is introduced due to the non-symmetry of equation 3, causing the left ϕ^l and right ϕ^r eigenvectors to be different. In this case the following special relation exists between both eigenvectors (see e.g. Ref. 4):

$$\phi_i^l = \begin{pmatrix} \phi_{si}^r \\ \dfrac{1}{\omega_i^2}\phi_{fi}^r \end{pmatrix} \tag{13}$$

provided that the eigenvalue ω_i^2 not equals zero (rigid body mode).
In case of a fluid rigid body mode the left eigenvector yields:

$$\phi_i^l = \begin{pmatrix} 0 \\ \phi_{fi}^r \end{pmatrix} \tag{14}$$

In case of a structure rigid body mode the left eigenvector depends on the inverse of the fluid stiffness matrix (Ref. 4) and is expensive to solve. However, in a normal application rigid body modes of the structure are not present or can easily be avoided by selecting appropriate boundary conditions.

11. Solve the modal fluid-structure response problem obtained in the previous step for the frequency domain of interest. This can be done fast, since the matrices are in terms of modal co-ordinates and thus small. In general, the modal matrices will not be diagonal matrices, but banded, since the undamped uncoupled modes will not be a perfect basis for the coupled problem. Also the matrices are non-symmetric, due to the couple terms. Therefore, standard modal methods cannot be applied, instead a direct method has to be used, which still is fast given the small size of the modal matrices.

2.2.2 Calculation of the response of the fluid domain and derived quantities

12. Determination of the fluid response P_f due to structural vibrations U_s, i.e. second row in equation 3

$$(K_f + i\omega D_f - \omega^2 M_f)P_f = \omega^2 C_{fs}H_{fs}U_s \qquad (15)$$

Here D_f is the fluid damping matrix, representing the impedance end-boundary condition. Because of this, a modal approach cannot be applied. A direct approach has to be used instead, which is an expensive step, depending strongly on the mesh density of the fluid domain. The same is true when a BEM approach is applied.

13. Calculation of derived quantities such as: sound intensity and transmission loss, which is a post-processing step and not computationally expensive. More details are given in the next section.

2.3 Sound Intensity and Transmission Loss

The goal of the analysis is to calculate the amount of energy transmitted through a fuselage structure and is expressed as the **Transmission Loss** (TL), defined by:

$$TL = 10\log_{10}\left(\frac{1}{\tau}\right) = 10\log_{10}\left(\frac{E_{inc}}{E_{trans}}\right) \qquad (dB) \qquad (16)$$

in which τ is the **transmission coefficient** defined as the ratio of the transmitted sound power E_{trans} and the incident sound power E_{inc}, which is a measure how well sound is passing from one volume to another through an intervening partition.

The **sound power** E is the amount of energy flowing through a control surface in the fluid domain A per second and can be found by integration of the sound intensity over the surface.

$$E = \int_A I(\underline{x})dA \qquad (W) \qquad (17)$$

where the (active) sound intensity in a point $\underline{x}$ is defined as the time average of the pressure fluctuation times the velocity:

$$I(\underline{x}) = \frac{1}{T}\int_t p(\underline{x},t)\,\underline{v}(\underline{x},t)dt = \frac{1}{2}\text{Re}\left(P\underline{V}^*\right) \qquad (W/m^2) \qquad (18)$$

where P and $\underline{V}$ represent the complex amplitudes in case of a sinusoidal sound field. The superscript * stands for the complex conjugate.

The fluid domain is formulated in terms of pressure (fluctuation). The velocity can be obtained from the linearised Euler's equation (conservation of momentum), which yields for a sinusoidal sound field:

$$\underline{V} = \frac{\hat{i}}{\omega\rho}\nabla P = \frac{\hat{i}}{\omega\rho}\frac{P_2 - P_1}{\Delta} \qquad (19)$$

Calculation of the velocity thus requires the gradient of the pressure, which is determined by a first-order finite difference scheme using two grids of points some distance apart (called field point mesh), schematically depicted in figure 1.1, denoted by the indices 1, respectively, 2. This is equivalent as what is done in sound intensity measurements using a sound intensity probe consisting of two microphones measuring the pressure at two points a distance Δ apart. Δ should be selected much smaller than the smallest wavelength of interest and is a high frequency limitation. This poses no limitation for a FEM analyses, because the wavelengths that can be

analysed are limited by the mesh size and modal density. The field point surface may be selected anywhere in the fluid domain and the pressure at the grid points can be obtained from the known pressure response values in the surrounding fluid element nodes.

Equivalently, for the pressure amplitude the mean complex pressure is used:

$$P = \frac{P_2 + P_1}{2} \tag{20}$$

Combining the above three equations yields the sound intensity in a direction x:

$$I_x = \frac{-1}{4\omega\rho\Delta}\text{Re}\left((P_1 + P_2)\hat{i}(P_2^* - P_1^*)\right) = \frac{1}{2\omega\rho\Delta}\text{Im}(P_1 P_2^*) = \frac{1}{2\omega\rho\Delta}(P_{2r}P_{1i} - P_{1r}P_{2i}) \tag{21}$$

The indices r and i denote the real, respectively, imaginary part of the pressure.

The (active time averaged) sound intensity thus depends on the phase difference between the pressure values in the two field points, introduced by energy dissipation in the FEM model. A small active intensity component, compared to the pressure, can cause numerical as well as experimental problems. For a strongly reactive field two more or less equal numbers are subtracted. This causes a loss of accuracy, since the accurate digits are subtracted leaving a zero for these digits.

The total sound power E (Eq. 17) now is obtained by integrating the intensity over a control surface. The field point mesh hereby consists of N equal sub-domains. The surface integration thus becomes the following simple summation:

$$E = \sum_{ip=1}^{np} I_{ip}\, dA_{ip} = \frac{A}{N}\sum_{ip=1}^{np} I_{ip} = A\, I_{mean} \qquad \text{(W)} \tag{22}$$

In order to determine the transmitted sound power E_{trans} in the receiving domain the total pressure first has to be separated into a forward (transmitted) and backward (reflected) travelling wave.

$$P = P_{trans} + P_{ref} = P_{trans}'\, e^{-\hat{i}kx} + P_{ref}'\, e^{\hat{i}kx} \tag{23}$$

This can be easily obtained from the sound pressures at the two points of the field point mesh, which yields:

$$P_{trans}' = \frac{P_1\, e^{\hat{i}kx_2} - P_2\, e^{\hat{i}kx_1}}{e^{\hat{i}k\Delta} - e^{-\hat{i}k\Delta}} \quad ; \quad P_{ref}' = \frac{-P_1\, e^{-\hat{i}kx_2} + P_2\, e^{-\hat{i}kx_1}}{e^{\hat{i}k\Delta} - e^{-\hat{i}k\Delta}} \tag{24}$$

The total incident sound power E_{inc} is determined by assuming a plane wave condition at each structural element and sum all contributions for the elements within the control surface:

$$E_{inc} = \sum_{ielm=1}^{nelm} \frac{P_{inc_{ielm},r}^2 + P_{inc_{ielm},i}^2}{2\rho c} A_{ielm} \quad \text{(W)} \tag{25}$$

The pressure loading applied in the FEM analysis represent the total pressure ($P_{inc} + P_{ref}$). Assuming a reflection coefficient ($r = P_{ref}/P_{inc}$) of 1 means the power has to be divided by a factor of 2. This only is true in an approximate sense. For low frequencies (below 200 Hz according to the mass law) this will not be correct, as well as for some specific resonance frequencies above the 200 Hz.

Finally, knowing E_{inc} and E_{trans} the transmission loss can be determined according to equation 16.

2.4 Glass wool model

The most extensive theory available to model the glass wool in the furnished configuration is the Biot theory (Ref. 5). Here, both the porous media and the fluid are modelled separately,

including the coupling between the two domains. Besides the fact that the theory is quite complex, it is not applicable here to model the glass wool. This, because the stiffness of the fibre-matrix is very low (it can be compressed easily) and therefore the model suffers from many very low frequency fibre-matrix modes, which makes it unsuitable for a FEM approach.

A much better approach here is the Limp theory (Ref. 6) neglecting the fibre-matrix stiffness. As a consequence the model is not capable to detect resonances in the porous media. This poses some limitations on the use of the model: the acoustic wavelength should be larger than the thickness of the porous layer. Another assumption is that the material is regarded as homogeneous. This assumption is valid if the size of the pores is much smaller than the acoustic wavelength. Both are valid assumption here, since the thickness of the glass wool layer is approximately 5 cm and thus the limiting frequency about 290/(2*0.05) = 2900 Hz, which is much higher than the frequency domain analysed (up to 1000 Hz), see chapter 3.

The Limp model results in the Helmholtz equation with a complex wave number.

$$\nabla^2 p + k_p^2 p = 0 \quad ; \quad k_p^2 = \left(\frac{\omega}{c_p}\right)^2 f(\omega) \quad ; \quad f(\omega) = K_s - \frac{\dfrac{i\phi h}{\omega \rho_f}}{1 - \dfrac{i\phi h}{\omega(1-h)\rho_s}} \tag{26}$$

with,

K_s	= 1		Structure factor
H	= 0.99		Porosity (volume percentage pores in material)
Φ	= 38000	Ns/m^4	Viscous flow resistance
ρ_s	= 2190	kg/m^3	Fibre density
ρ_f	= 1.2	kg/m^3	Fluid density (air at room temperature)
c_p	= 290	m/s	Isothermal sound speed (air at room temperature)

The structure factor accounts for the effect of inaccessible pores and can be taken K_s=1 for glass wool. The value for the porosity and viscous flow resistivity have been obtained by measurements performed by University of Oldenburg.

The Limp model has been implemented in B2000. The "stiffness" matrix is complex and frequency dependent. The glass wool thus is assumed to behave like a viscous fluid. The frequency dependency is hard (expensive) to solve, therefore the complex coefficient is determined for the frequency half way the frequency interval analysed, i.e. 500 Hz, and kept constant over the whole frequency domain.

3 Numerical results for an Aluminium fuselage panel

In this chapter the numerical results are presented obtained with the solution strategy discussed in the previous chapter, applied to an Aluminium fuselage panel. The panel has been analysed for the following configurations:

- Bare
- Damped (a damping layer has been added, see figure 3.1 left picture)
- Damped and furnished (besides the damping layer a glass wool blanket has been added, see figure 3.1 right picture)

The fuselage panel was 2.22 m long and 1.54 m in circumfential direction.

Figure 3.1: Damped (left) and furnished (right) Aluminium fuselage panel

In the next sections first the model of the experimental set-up at NLR, schematised in figure 3.2, will be discussed. This set-up consists of the test structure (fuselage panel), a reverberation room on one side, in which the sound field is generated and a receiving (semi-anechoic) room on the other side, in which the transferred sound field is measured. The last is done by scanning a control surface (bounded by duct) with a sound intensity probe.

In this case, the influence of the fluid on the dynamical behaviour of the panels is small (weak fluid-structure coupling), due to size, high stiffness and mass of the structure. Therefore, in the calculation of the response of the panels due to the impinging sound field (first part of the analysis scheme, section 2.2.1) the fluid-structure coupling could be neglected. However, the reverberation room still was modelled to predict the incident sound field impinging on the structure (section 3.1). The fluid-structure interaction on the receiving side was modelled to determine the sound radiation (section 3.2).

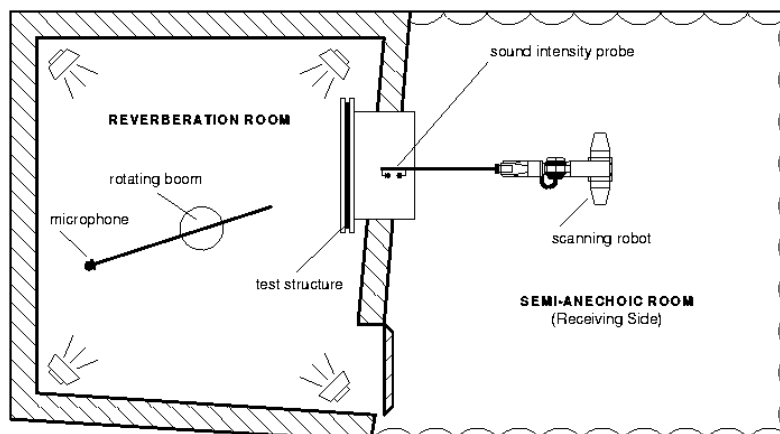The frequency domain of interest was 0..1000 Hz.

Figure 3.2: Schematised measurement set-up, from Ref. 7

3.1 Reverberation room

In the experimental set-up, schematised in figure 3.2, use is made of a reverberation room to generate a diffuse sound field. However, according to Schroeder's equation the dimensions of the room are such that the sound field is not diffuse for frequencies below 500 Hz, i.e.:

$$f_c = \sqrt{\frac{6c^3 T_{60}}{55.3V}} = \sqrt{\frac{6*340^3*2}{55.3*33.4}} = 505\,\text{Hz} \tag{27}$$

T_{60} is the reverberation time and V the volume of the room.

This was the reason to model the room, since it concerns a significant part of the frequency domain in the FEM TL-analysis and is also the most important part for sound reduction. The objective was to determine an approximation of the sound field that impinges on the panels, in order to improve the validation of the FEM results.

Figure 3.3 shows the FEM model of the reverberation room, including the noise sources: four loudspeakers near the corners of the room and a dodecahedron placed at successively 3 different positions to generate sufficient sound power below 500 Hz. The volume has been modelled with 10*10*10 quadratic elements. The mesh density is not sufficient to cover the whole frequency domain of interest (up to 1000 Hz), however, this is not regarded as a real limitation, since the sound field should only approximate a diffuse kind of sound field above 500 Hz.
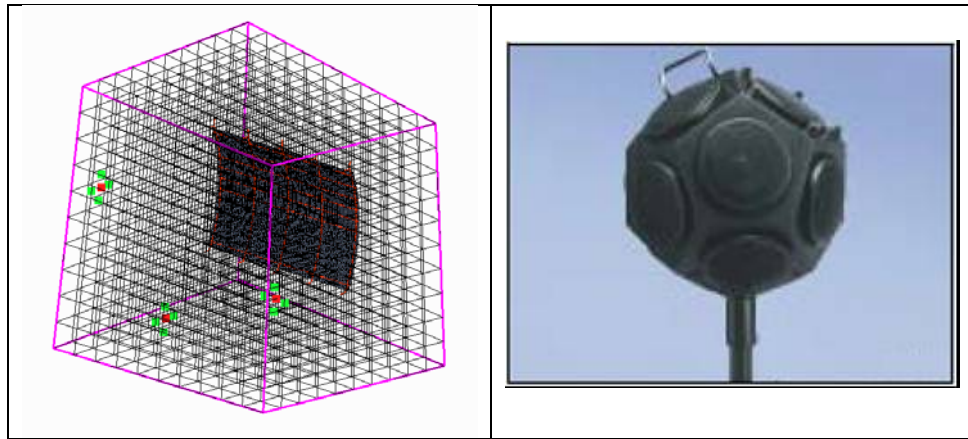

Figure 3.3: Left: FEM model of reverberant room including the FEM model for the Aluminium fuselage panel. Red spots are the dodecahedron source positions. Right: dodecahedron.

The fluid response at the panel determines the incident field and is calculated for each frequency for which the transmission loss is determined later on.

In the response analysis damping has been included to model the reverberation time. This will result in a complex frequency dependent sound field. In the frequency range of interest (100 up to 1000 Hz) the reverberation time T_{60} is on average 1.5 seconds. This value has been used to determine an appropriate damping value. The time dependent pressure at a point can be written as:

$$p(t) = p(t_0)e^{-\delta t} = p(t_0)e^{-\frac{\alpha}{2}t} \tag{28}$$

In which δ (=$6.9/T_{60}$) is the reverberation constant and α the Rayleigh damping coefficient (D= $\alpha M + \beta K$). This damping coefficient α thus has a value of 9.2.

The response analysis included all sources simultaneously to arrive at an average sound field (similar as is done for measurement results). The same source level was applied at all frequencies to approximate the white noise of the dodecahedron. Since the transmission loss is a ratio of the incident and transmitted sound power, the absolute level of the sources was not important. Furthermore, a direct instead of a modal method was applied to determine the complex response. A modal approach could not be applied due to the high modal density in the frequency range of interest (up to 1000 Hz) , already more than 500 roots in the interval 0 to

17

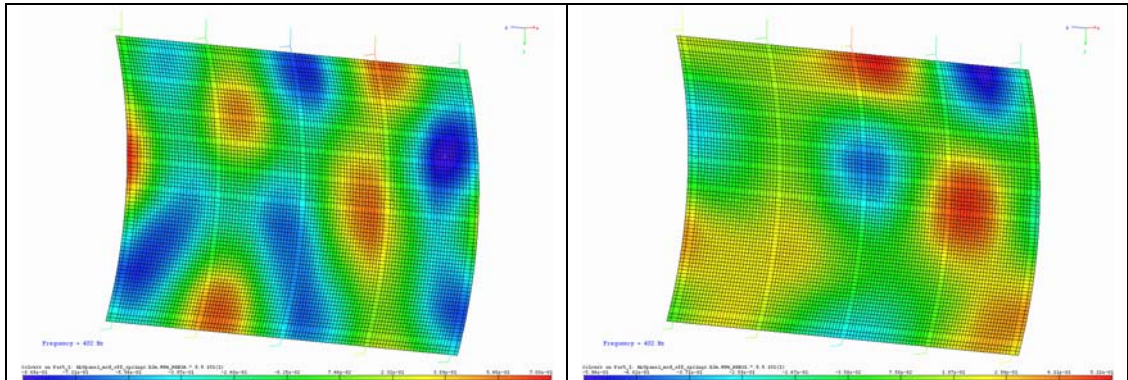500 Hz. Figure 3.4 depicts an example of the resulting pressure distribution on the panel at 402 Hz.

Figure 3.4: Complex frequency dependent pressure distribution at the panel, real (left) and imaginary (right) part, for 402 Hz

3.2 Receiving room

The receiving room consisted of a duct in which the sound intensity was measured and a semi-anechoic room behind it, see figures 3.2 and 3.5. Therefore, it was regarded sufficient to model only the duct with an impedance value at the far end as shown in figure 3.5, which also depicts the FEM mesh used. The impedance value applied was $\rho*c$, approximating the Sommerfeld radiation condition, in order to prevent reflection at the end of the Duct as much as possible. The mesh density was 21*20*20 linear acoustic elements, which is much coarser than the panel meshes. The mesh is fine enough to accurately represent the pressure distributions due to the panel vibrations.
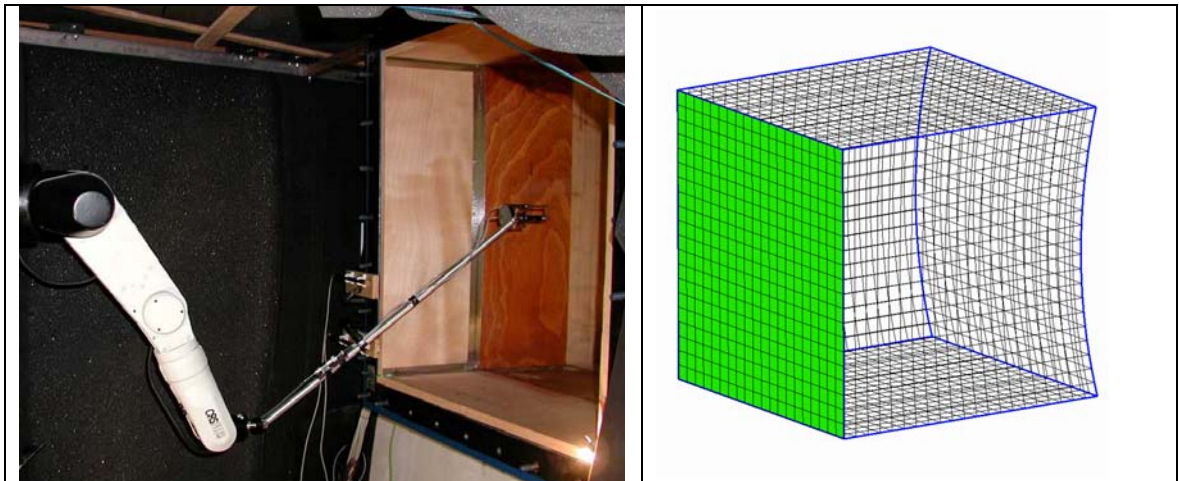

Figure 3.5: Sound intensity measurement set-up (left) and FEM mesh of duct with impedance boundary condition (green) representing the end-plane

3.3 Aluminium fuselage panel

Figure 3.6 shows the FEM mesh of the fuselage panel (for the damped configuration) consisting of: shell elements (light blue), beams elements (red) and rods elements (green). The rods represent the springs used in the experimental set-up to suspend the panel. All degrees of

freedom have been locked at the end nodes of the rods (springs). Furthermore, the rotation around the normal (drill) has been locked for all shell element nodes not coinciding with a beam node, to remove the singularity associated with this degree of freedom. For this node-local co-ordinate systems have been allocated to these nodes.

Some model characteristics are: 9711 elements (1184 beams and 15 rods), 8721 nodes and 44766 degrees-of-freedom.
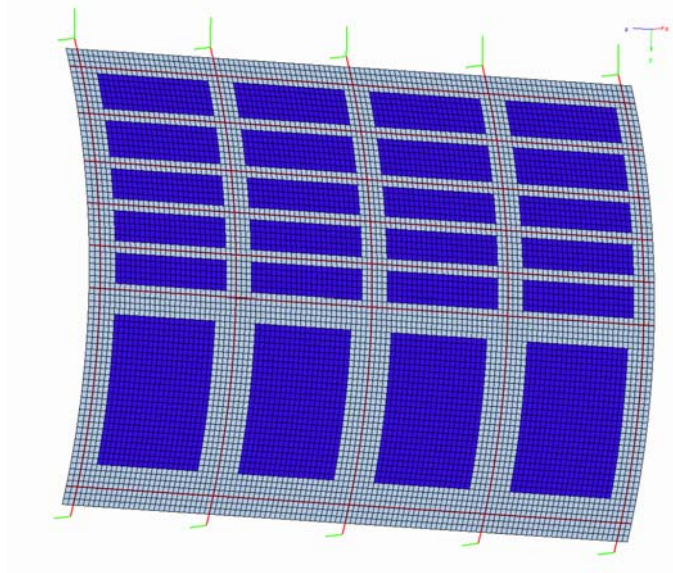

Figure 3.6: FEM mesh of the damped Aluminium panel: shells (light blue), beams (red) and rods (green). The dark blue elements represent the constrained layer damping.

3.3.1   Modal analysis of bare fuselage panel

First a modal basis was computed. It was decided to take into account the first 400 modes (up to 1100 Hz), which means that the response is accurate up to approximately 1000 Hz. The first six modes are rigid body modes (spring modes) and the seventh is the first real panel mode. Figure 3.7 depicts one of the lowest and highest mode shapes. For some of the highest modes the mesh density becomes very coarse.
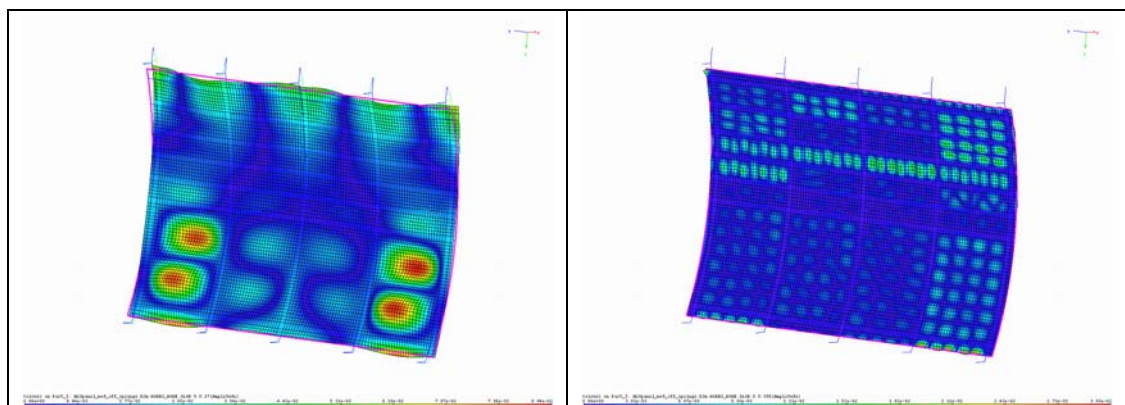

Figure 3.7: One of the lowest (17th) and highest mode shapes (390th).

To validate the FEM model, the calculated mode shapes and eigenfrequencies were compared with the experimental results obtained from a modal analysis (Ref. 7). The Modal Assurance Criterion (MAC) was applied to compare the mode shapes:

$$MAC_{ij} = \frac{\left|\phi_i^{num} \cdot \phi_j^{exp}\right|^2}{\left(\phi_i^{num} \cdot \phi_i^{num}\right)\left(\phi_j^{exp} \cdot \phi_j^{exp}\right)} \tag{29}$$

A MAC value of 1 indicates a fully correlated mode shape. In table 3.1 the MAC values (column 3) are presented for all measured experimental modes (column 1) together with the best correlating numerical mode (column 2). Overall the correlation is excellent, which can also be seen from the modal plots in figure 3.8. For some modes the correlation is low, but in all cases the quality of the measured mode then is questionable. Furthermore, not all numerical modes were detected in the measurement. The excellent correlation is also found for the corresponding eigenfrequencies, depicted in figure 3.9. In the ideal case all the points would have been on the red-line. The deviation becomes lager for the higher modes.
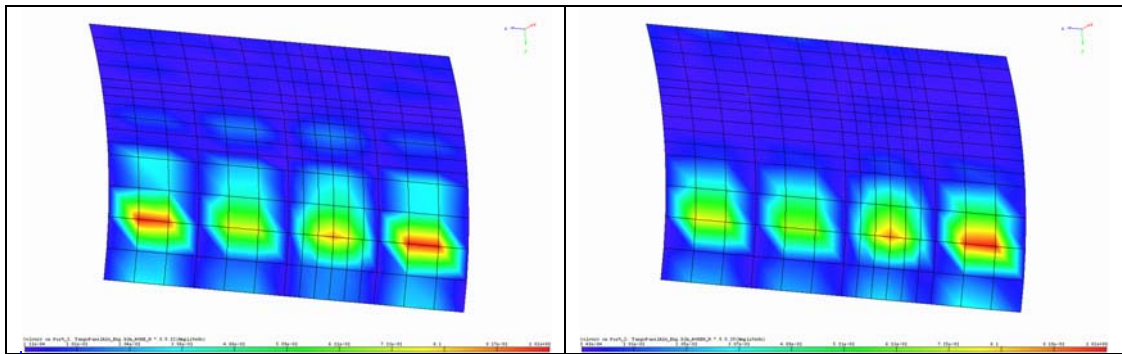

Figure 3.8: Experimental (left) versus numerical (right) mode shape on the experimental grid: mode 12

Exp. Mode nr.	Num. Mode nr.	MAC	Exp. Freq	Num. Freq	Exp. Mode nr.	Num. Mode nr.	MAC	Exp. Freq	Num. Freq
1	8	0.96	44.7	46.0	14	22	0.84	179.4	196.8
2	9	0.90	99.2	99.9	15	25	0.51	185.6	200.2
3	10	**0.41**	102.9	103.0	16	37	**0.30**	194.7	245.2
4	9	**0.36**	107.7	99.9	17	35	0.59	213.8	240.9
5	12	0.56	110.8	114.2	18	48	**0.28**	220.5	296.3
6	11	0.71	118.6	111.6	19	48	0.60	235.7	296.3
7	13	**0.36**	140.6	138.0	20	45	**0.34**	242.6	285.7
8	13	0.57	145.8	138.0	21	49	0.60	246.9	303.9
9	18	0.79	153.4	175.6	22	48	**0.44**	256.9	296.3
10	14	0.59	157.1	146.6	23	47	0.80	267.2	289.2
11	19	0.59	162.5	178.5	24	53	**0.24**	275.2	316.2
12	20	0.89	168.9	190.8	25	52	0.64	277.5	315.9
13	21	0.54	173.0	190.9	26	57	0.57	288.1	328.8

Table 3.1: MAC numbers and eigenfrequencies (Hz) for the experimental and numerical modes of the bare Aluminium panel
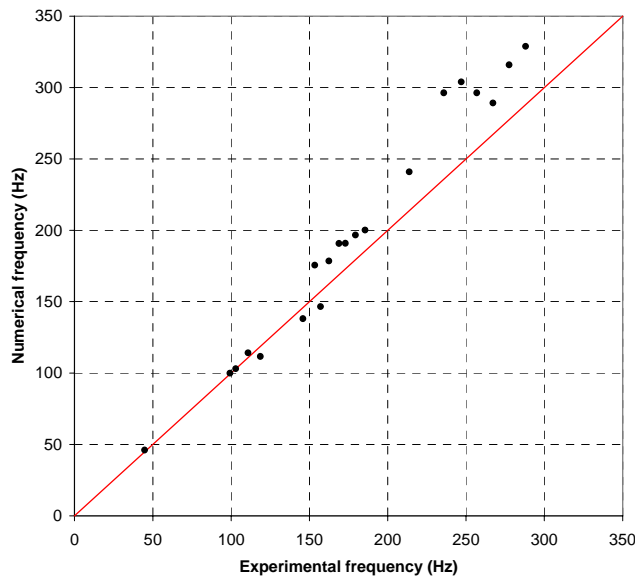
Figure 3.9: Numerical versus experimental eigenfrequencies for Aluminium panel

3.3.2 Response analysis

After determination and validation of the structure modes, see previous section, the next step in the TL-analysis was the calculation of the response of the structure (see section 2.2.1) for all three configurations, caused by the incident complex frequency dependent pressure field discussed in section 3.1.

Bare configuration

For the bare panel a modal damping value ξ of 0.001 was applied to model the damping. This value is based on the damping measured in the modal analysis, for which a mean damping value of 0.001 was found.

Damped configuration

For the damped configuration (see figure 3.1 and 3.6) the FEM model was modified. Two extra layers were added to the model for the shell elements located at the places where the damping tape was attached, see figure 3.6. The damping tape (Soundfoil type 15LT12) consisted of a 0.18 mm visco-elastic layer and a 0.38 mm thick Aluminium layer (constraining layer damping). The visco-elastic damping layer was modelled as a layer with low stiffness and complex modulus (E and G). The following properties have been selected, based on experiments performed by the University of Oldenburg:

E = 5 GPa v = 0.3 β = 0.3

The loss factor β is defined as the ratio of the imaginary and real part of the young's or shear modulus. The loss factor is frequency dependent. This frequency dependency is hard (expensive) to solve, therefore a mean value of 0.3 over the frequency range of interest (0 to 1000 Hz) was chosen. The density of the visco-elastic layer can be neglected.

Furnished configuration

For the furnished configuration the Limp glass wool model, as discussed in section 2.4, was applied. In the experimental set-up the glass wool is located on the incident side of the panel, depicted in the picture on the right of figure 3.1. The mass and stiffness of the glass wool is very low and therefore it has a neglectable effect on the dynamical behaviour of the panel. Its main contribution comes from reducing the incident field, due to the viscous behaviour of the glass wool. Therefore, in the numerical model the glass wool has been modelled as a 5 cm thick layer

on the receiving side of the panel, see figure 3.10, which should have the same effect on the transmission loss of the panel. In this way the size of the numerical model is reduced considerable. The number of elements is strongly reduced, since the fluid mesh is much coarser and also covers a smaller area than the structure mesh.
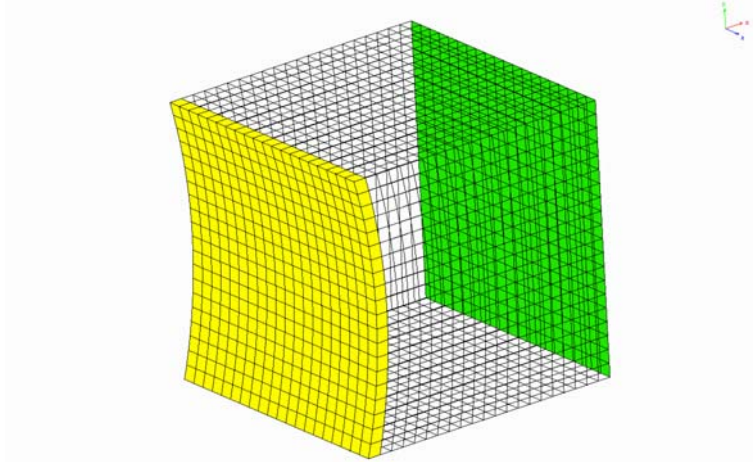

Figure 3.10: FEM model Duct with glass wool layer (yellow) and impedance boundary condition (green)

3.3.3 Transmission Loss analysis
Knowing the response of the panel the next step was the determination of the sound radiation caused by it (see section 2.2.2). For this, the fluid-structure interface was determined, shown in figure 3.11 by the purple rectangular, in which the non-coinciding mesh on the interface is clearly shown.
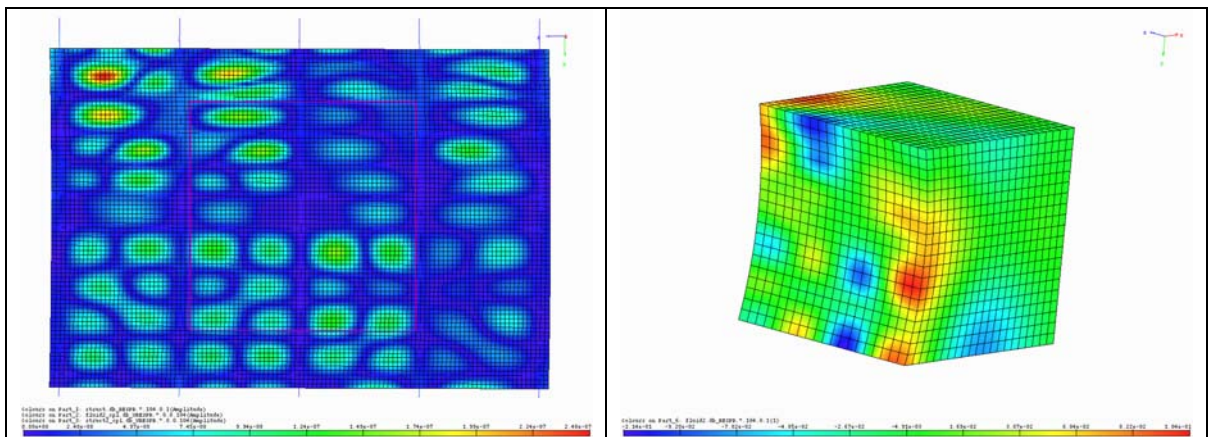

Figure 3.11: Response at 414 Hz for: panel displacement (left) and resulting fluid response in duct (lower right)

Based on the response of the panel, the response in the duct (receiving fluid domain) was determined, see section 2.2.2. A typical result (for 414 Hz) is depicted in figure 3.11. In the left picture the panel response is depicted caused by the complex incident pressure field (U_s in equation 15). The resulting fluid response in the duct is shown in the right picture (P_f in equation 15). From this fluid response the transmission loss and other quantities were determined, as explained in section 2.3. The field point mesh, schematically depicted in figure 1.1, at which the sound intensity and other quantities are obtained, was located at the same position in the duct as the sound intensity probe in the experimental set-up, i.e. 135 mm from the end of the duct. The

field point mesh consisted of two planes 1 mm apart, each containing 21*21 equidistant points. Figure 3.12 depicts the sound field at the field point mesh for a characteristic result (at 836 Hz).
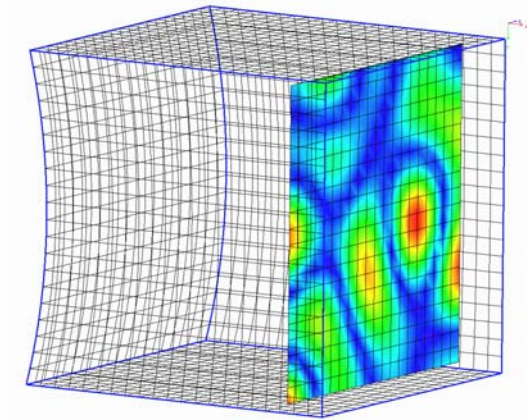

Figure 3.12: Calculated sound field at 836 Hz on the field point mesh: real part of the total pressure

Finally, figure 3.13 depicts the transmission loss curves. The figure shows the measured (dotted lines) and calculated (drawn lines) curves for the three configurations analysed: bare, damped and furnished. For all three configurations the correlation is excellent for frequencies above the 350 Hz (less than 2 dB differences). Below the 350 Hz, a much higher TL is predicted in the numerical analyses. This can be due to: spring attachment (causing rigid body modes of the panel); loss of accuracy due to low system damping; errors in the calculated incident sound field, a reflection coefficient of one will not be a good approximation for low frequencies.
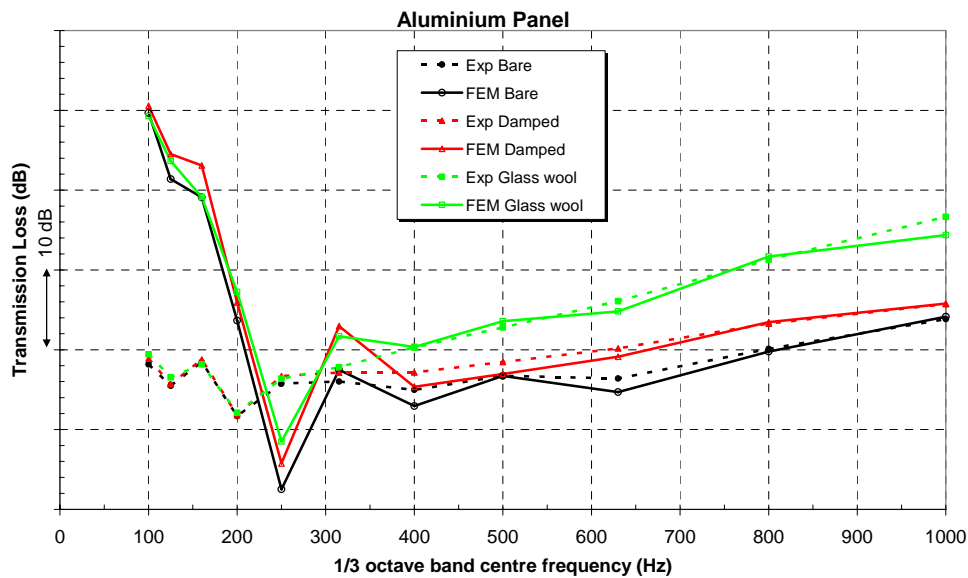

Figure 3.13: Experimental (dotted) and numerical (solid) TL-curves for Aluminium panel configurations: bare, damped and furnished

4 Conclusions

A new approach has been presented in detail to solve structural-acoustic problems. The structure as well as the fluid is modelled with the Finite Element Method. The new approach reduces the computational effort compared with a more conventional FEM approach. This is necessary in case of large models, existing for realistic aircraft structures such as fuselage panels or even a fuselage barrel, which are the structures analysed within the framework of FACE. The main objective here was to predict the sound transmission (TL) through these realistic aircraft fuselage panels.

Results obtained with this approach are presented for a bare, damped (viscous constraining layer) and furnished (glass wool) large Aluminium fuselage panel configuration. The results have been compared with experimental data (modal and TL-data), validating the approach.

For the Aluminium fuselage panel the correlation with the experimental transmission loss results is excellent for frequencies above the 350 Hz (less than 2 dB differences). Below the 350 Hz, a much higher TL is predicted in the numerical analyses. This can be due to errors in the calculated incident sound field, e.g. wrong value of the reflection coefficient.

Similar results have been obtained for a Composite fuselage panel, although the correlation with experimental TL results was somewhat less than for the Aluminium panel, but still good for frequencies above the 400 Hz.

References

[1] S. Merazzi, *Modular finite element analysis tools applied to problems in engineering*, PhD thesis 1251 of the EPFL Lausanne Switzerland, 1994

[2] W.M. Beltman, *Viscothermal wave propagation including acousto-elastic interaction*, PhD thesis, University of Twente, The Netherlands, ISBN 90-365-1217-4, 1998

[3] T.Y. Rong and A.Q. Lu, *Generalized mixed variational principles and solutions of ill-conditioned problems in computational mechanics. Part II: Shear locking*, Comput. Methods Appl. Mech. Engrg., Vol. 192, pp. 4981-5000, 2003

[4] Z.D. Ma and I. Hagiwara, *Development of a new mode-superposition technique for modal frequency response analysis of coupled acoustic-structural systems*, Finite Element in Analysis and Design, Vol. 14, pp. 209-223, 1993

[5] M.A. Biot, *Generalized theory of acoustic propagation in porous dissipative media*, Journal of the acoustical society of America, 34(9), pp. 1254-1264, 1962

[6] K.U. Ingard, *Locally and non-locally reacting flexible porous layers; a comparison of acoustical properties*, A.S.M.E. transactions journal of engineering for industry, 103, pp. 302-313, 1981

[7] H.M.M. van der Wal and A.C. Nilsson, *Sound-transmission measurements on composite and metal fuselage panels for different boundary conditions*, National Aerospace Laboratory NLR, NLR-TP-2005-570, 2005